

A deep submillimetre survey of the Galactic Centre

D. Pierce-Price¹, J. S. Richer¹, J. S. Greaves², W. S. Holland², T. Jenness², A. N. Lasenby¹, G. J. White^{3,1}, H. E. Matthews^{4,2}, D. Ward-Thompson⁵, W. R. F. Dent⁶, R. Zylka⁷, P. Mezger⁸, T. Hasegawa⁹, T. Oka¹⁰, A. Omont¹¹ and G. Gilmore¹²

ABSTRACT

We present first results from a submillimetre continuum survey of the Galactic Centre ‘Central Molecular Zone’ (CMZ), made with SCUBA on the James Clerk Maxwell Telescope. SCUBA’s scan-map mode has allowed us to make extremely wide-field maps of thermal dust emission with unprecedented speed and sensitivity. We also discuss some issues related to the elimination of artefacts in scan-map data. Our simultaneous 850/450 μ m maps have a total size of approximately $2.8 \times 0.5^\circ$ (400 \times 75 pc) elongated along the galactic plane. It covers the Sgr A region—including Sgr A*, the circumnuclear disc, and the +20 km/s and +50 km/s clouds; the area around the Pistol; Sgr B2—the brightest feature on the map; and at its Galactic Western and Eastern edges the Sgr C and Sgr D regions. There are many striking features such as filaments and shell-like structures, as well as point sources such as Sgr A* itself. The total mass in the Central Molecular Zone is greater than that revealed in previous optically-thin molecular line maps by a factor of ~ 3 , and new details are revealed on scales down to 0.33 pc across this 400 pc-wide region.

¹Cavendish Astrophysics, Cavendish Laboratory, Madingley Road, Cambridge, CB3 0HE, UK

²Joint Astronomy Centre, 660 N. A‘ohōkū Place, Hilo, HI 96720

³Department of Physics, Queen Mary and Westfield College, University of London, Mile End Road, London E1 4NS, UK

⁴National Research Council of Canada, Herzberg Institute of Astrophysics, 5071 West Saanich Road, Victoria, BC V9E 2E7, Canada

⁵Department of Physics and Astronomy, Cardiff University, 5 The Parade, Cardiff CF2 3YB, Wales, UK

⁶Astronomy Technology Centre, Blackford Hill, Edinburgh, EH9 3HJ, UK

⁷ITA, Universität Heidelberg, Tiergartenstrasse 15, D-69121 Heidelberg, Germany

⁸Max-Planck-Institut für Radioastronomie, Auf dem Hügel 69, D-53121 Bonn, Germany

⁹Institute of Astronomy, University of Tokyo, 2-21-1 Osawa, Mitaka, Tokyo 181-0015, Japan

¹⁰Department of Physics, Graduate School of Science, The University of Tokyo, 7-3-1 Hongo, Bunkyo-ku, Tokyo 113-0033, Japan

¹¹Institut d’Astrophysique de Paris, CNRS, 98bis Boulevard Arago, F 75014 Paris, France

¹²Institute of Astronomy, University of Cambridge, Madingley Road, Cambridge. CB3 0HA, UK

Subject headings: Galaxy: center — ISM: clouds — ISM: structure — dust, extinction — techniques: image processing — submillimeter

1. Introduction

The Galactic Centre provides our best opportunity to study the astrophysical processes in a galactic nucleus with high spatial resolution. These include star-formation and the molecular cloud structures in a region subjected to strong shear forces, magnetic fields, and gravitational potentials. Thermal dust continuum emission traces the temperature-weighted column density of material in a less biased way than molecular line maps, which are affected by excitation, optical depth, and abundance variations. Thus, we can use the continuum emission to map the mass distribution in molecular clouds with good accuracy and sensitivity.

We used SCUBA (Holland et al. 1999) on the 15-m James Clerk Maxwell Telescope (JCMT), between April 1998 and April 2000, to map the Galactic Centre region in the submillimetre continuum at $450\,\mu\text{m}$ and $850\,\mu\text{m}$. The new images cover a region 4 times larger and ~ 100 times deeper than earlier surveys (Lis & Carlstrom 1994). The map size is approximately $2.8 \times 0.5^\circ$, or $400 \times 75\,\text{pc}$ at an assumed distance of $8.5\,\text{kpc}$. The map covers the entire ‘Central Molecular Zone’ (CMZ), which extends to radii of $200\,\text{pc}$ and contains up to 10% of the Galaxy’s molecular interstellar medium (ISM) (Morris & Serabyn 1996).

2. Observations and data reduction

SCUBA (Holland et al. 1999) is a submillimetre continuum bolometer camera with two arrays, one of 91 pixels optimised for $450\,\mu\text{m}$, and one of 37 pixels optimised for $850\,\mu\text{m}$. In use, both arrays observe simultaneously. The resolution is $8''$ FWHM at $450\,\mu\text{m}$ and $15''$ at $850\,\mu\text{m}$.

SCUBA was used in scan-map mode, in which the array is scanned across the sky at a rate of $24''$ per second whilst chopping the secondary mirror at 7.8 Hz. This chopping produces images in which the sky is convolved with the primary beam of the telescope and a dual-beam function, of positive and negative delta functions separated by the chop throw.

The majority of the map was observed six separate times, with chop throws of 20, 30, and $65''$ in both R.A. and Dec., although some fields at the Galactic Eastern and Western ends were observed with 30, 44, and $68''$ chops. Each dual-beam image contains no information at spatial frequencies equal to the inverse chop throw and its harmonics, and the constant power level (zero spatial frequency) is also lost.

The data were reduced with SURF, the standard SCUBA reduction software (Jenness & Light-

foot 1999), using the “Emerson 2” deconvolution algorithm. This algorithm combines the multiple chop-throw images of the map fields. A weighted average of these observations is formed in Fourier space, and the reverse transform yields the final map (Jenness & Lightfoot 1998). Although the combination of multiple chops improves the spatial frequency coverage, it is unavoidable that spatial scales more extended than a few times the maximum chop-throw are measured with reduced sensitivity, and the zero spatial frequency is still lost. Ultimately, the survey is sensitive to spatial scales in the approximate range 0.3 pc (the beam size at $450\mu\text{m}$) to ~ 10 pc (a few times the maximum chop-throw).

Calibration was performed from maps of Uranus and Mars, and all data were corrected for atmospheric extinction using skydips. Zenith opacities were in the range 0.1–0.45 at $850\mu\text{m}$ and 0.33–2.5 at $450\mu\text{m}$. Most of the data in the central 1.5° region was observed in extremely good weather, with $\tau(850\mu\text{m}) < 0.13$, $\tau(450\mu\text{m}) < 0.5$.

To calibrate fluxes of extended structures, the integrated signal in a $1'$ diameter aperture was used to calculate a conversion factor in $\text{Jy arcsec}^{-2} \text{V}^{-1}$. Calibration relative to the primary calibrators is estimated to be accurate to 5% at $850\mu\text{m}$ and 20% at $450\mu\text{m}$, based on the dispersion of measured flux conversion factors, although absolute cloud fluxes also depend on corrections for constant map offsets as described in section 2.1.

The survey has resolutions of approximately $8''$ at $450\mu\text{m}$ and $15''$ at $850\mu\text{m}$, corresponding to distances of 0.33 pc and 0.62 pc at a distance of 8.5 kpc. The $1-\sigma$ sensitivities per beam are approximately 30 mJy and 300 mJy at $850\mu\text{m}$ and $450\mu\text{m}$ respectively, or $\sim 20 M_\odot$ per beam with the assumptions in section 3.5.

2.1. Corrections for artefacts

Making large-scale SCUBA scan-maps is difficult for several reasons. The total power level is not recorded, so there may be a constant offset on each field, and this offset may in general vary between fields in the mosaic. Within individual fields, one must account for baseline removal on the time-series signals from the bolometers. The dual-beam chop will suppress information at certain spatial frequencies, as described above, and as there is so much extended structure in the CMZ it is difficult to scan or chop onto regions of no emission.

Some previous SCUBA scan-maps have sometimes exhibited reduction artefacts, such as negative troughs around bright sources. We have found that negative troughs can be greatly reduced by careful baseline removal on a per-bolometer basis. A single $10' \times 10'$ map is constructed from typically 10–15 scans of the array across the field. Calculating a baseline separately for each scan will produce large spurious offsets for those scans which pass over bright structure, so ideally it is best to determine a baseline using only those scans which contain little bright emission. This proved impossible for a region as rich in structure as the Galactic Centre, but we have found that using the median level over all the scans for each bolometer does produce good results without the

spurious offsets.

This is the largest area ever scan-mapped at 450 and 850 μm , with more than fifty overlapping $10' \times 10'$ fields, which must be mosaiced to form the final image. The Starlink CCDPACK package (Draper, Taylor, & Allan 2000) was used to combine the dual-beam images and remove relative level offsets between fields of order 10 and 0.5 mJy arcsec $^{-2}$ at 450 and 850 μm respectively. We then applied further corrections to ensure that the pixel mean calculated along the chop throw direction was zero, for all of the mosaiced dual-beam maps. This must be true, as long as the edges of the map are essentially emission-free, and is necessary because incorrect zero levels in the mosaiced dual-beam maps will translate to slopes in the final images. We finally corrected for the constant zero offset on the entire map by measuring the typical zero levels from map areas devoid of identifiable clouds, and assigning an uncertainty based on the level variations. The final uncertainty in baseline levels is 15 and 1 mJy arcsec $^{-2}$ at 450 and 850 μm respectively, the former being higher in part due to the greater calibration uncertainties. These uncertainties have been neglected, compared to the sensitivity noise levels of the maps.

3. Analysis

3.1. General features

Our maps (figures 1 and 2) show good correspondence with previous surveys of the region, such as that by Lis & Carlstrom (1994) but with much higher sensitivity and resolution. At 850 μm we can clearly see the central source Sgr A* and its Circum-Nuclear Disc (CND) ($l = -0.05$, $b = -0.05$), although these features are less pronounced at 450 μm . We also see the compact GMCs M-0.13-0.08 (the +20 km/s cloud) and M-0.02-0.07 (the +50 km/s cloud). Close to this is the high-velocity molecular cloud CO 0.02–0.02 (Oka et al. 1999). At higher galactic longitude we see the Pistol region ($l = 0.15$, $b = -0.05$), other GMCs such as M0.25+0.01 (Lis et al. 1994), Sgr B1 ($l = 0.5$) and B2 ($l = 0.66$), and the Sgr D ($l = 1.1$) star-forming region. At more negative longitudes, the map extends to the Sgr C ($l = -0.5$) star forming region. All of the field is rich in extended structure, dominated by filamentary clouds and cavities which may be associated with supernova remnants. Such structures have also been observed by Oka et al. (1998) in CO ($J = 1-0$) emission.

3.2. Sagittarius A*

At both wavelengths we have a clear detection of the Sgr A* point-source. By taking slices through the position of Sgr A* to determine and remove the local background, we estimate the flux from Sgr A* itself, with quoted 1- σ uncertainties. The results are also subject to the overall calibration uncertainties described in section 2. At 850 μm we measure a flux of 2.6 ± 0.3 Jy. This

is consistent with the value measured from CSO-JCMT interferometry (Serabyn et al. 1997) of 3.2 ± 0.7 Jy. At $450\,\mu\text{m}$, the same procedure gives a flux for Sgr A* of 1.2 ± 0.4 Jy. This is consistent with the upper limit of 1.5 Jy found by Dent et al. (1993). These fluxes are somewhat lower than those measured by Zylka et al. (1995), which were 3.5 ± 0.5 Jy at $800\,\mu\text{m}$ (rather than $850\,\mu\text{m}$) and 3.0 ± 1.0 Jy at $450\,\mu\text{m}$, suggesting that there may be some variability of the Sgr A* point source. For example, Tsuboi, Miyazaki, & Tsutsumi (1999) observed a flare at 3mm during which the flux doubled, and Serabyn et al. (1997) found a flux of 7 ± 2 Jy at $350\,\mu\text{m}$. Our fluxes indicate a spectral index for the emission from Sgr A* of $-1.5^{+1.0}_{-1.4}$, consistent with a non-dust component in the emission. Flux values for the synchrotron component from the postulated black hole are discussed further by Aitken et al. (2000).

3.3. Greybody fitting

Although we can calculate spectral indices in the submillimetre regime from the SCUBA data, these data do not constrain the overall form of the dust emission, and do not allow us to estimate the temperature of the dust. To do this, we need data around the peak of the emission, which for dust at these temperatures is in the far infra-red.

We have combined our submillimetre data with $100\,\mu\text{m}$ data from the IRAS Galaxy Atlas (Cao et al. 1997), and fitted a single temperature greybody spectrum of the form $I_\nu = (1 - \exp(-\tau))B_\nu(T)$, where the optical depth τ is expressed in terms of an index β and a critical frequency ν_{crit} at which the emission becomes optically thick: $\tau = (\nu/\nu_{\text{crit}})^\beta$. Although the IRAS Galaxy Atlas also contains $60\,\mu\text{m}$ data, we believe that emission at this wavelength traces a higher temperature component. By fitting to the $850\,\mu\text{m}$, $450\,\mu\text{m}$, and $100\,\mu\text{m}$ points we calculate properties of the cold dust only.

We have performed a least-squares greybody fit to the three datasets over the survey area, fitting for temperature T and critical frequency ν_{crit} . We fixed $\beta = 2$, the theoretical maximum for crystalline dust grains. Since the resolution of the IRAS images was approximately $2'$, the SCUBA data were also smoothed to this resolution.

The fits indicate a fairly uniform dust temperature of $\sim 21 \pm 2$ K. There are no signs of strong temperature variations correlated with individual clouds, and this is further evidence that the brightness structure in the maps is dominated by column density variations. Therefore, we adopt a typical temperature of 20 K throughout the rest of this paper.

If β is allowed to vary, the fit is better but the derived temperature does not significantly change. Best-fit values of β are $\beta \sim 2.4$, higher than the canonical value of $\beta = 2$. There is now much evidence for $\beta > 2$: Lis & Menten (1998) and Dowell et al. (1999) measured $\beta \sim 2.8$ and $\beta \sim 2.5$ respectively in GCM0.25+0.01. In other regions, Lis et al. (1998) measure β values as high as 2.5 in the Orion Ridge and Bernard et al. (1999) also report PRONAOS observations of high β in the Polaris cirrus cloud. In laboratory work Koike et al. (1995) report β up to 2.7 in

carbon-based compounds at room temperature, and Agladze et al. (1996) have shown $\beta > 2$ in silicates between ≈ 5 and 20 K.

3.4. Spectral index map

We have used our 450 μm and 850 μm maps to generate a map of spectral index α (defined by $S_\nu \propto \nu^\alpha$), which is shown in figure 3. We first smoothed the 450 μm map to the lower resolution of the 850 μm observations, and imposed a lower threshold on both maps of $\sim 3\sigma$, since spectral indices derived from small flux values are subject to large errors.

Over most of the bright parts of the map α is in the range 3–4, indicating rather constant dust properties with a dust opacity index $\beta \sim 2$. The bulk spectral index for M-0.02-0.07 (the +50 km/s cloud) is $\alpha = 3.5 \pm 0.05$, whereas for M-0.13-0.08 (the +20 km/s cloud) it is $\alpha = 3.7 \pm 0.05$ (quoted errors are from the variation within the clouds). Assuming greybody emission at a dust temperature of 20 K, these indicate dust opacity indices of $\beta \sim 2.2$ –2.4. Although $\beta = 2$ is the theoretical upper limit for crystalline dust grains, in section 3.3 we discuss some evidence for higher values of β .

Differences in spectral index may be due to differences in temperature. Since at these temperatures, emission at 450 μm and 850 μm is not truly in the Rayleigh-Jeans part of the spectrum, the difference between the spectral index α and the dust opacity index β is temperature dependent. It is therefore possible that two clouds may have the same β but different temperatures, leading to different spectral indices. If this were the case, a lower α would indicate a cooler cloud. This cannot account for all the α variations: for example, α is *low* at only 3.2 ± 0.1 for CO 0.02-0.02, and this cloud is thought to be relatively *hot* at ~ 60 K (Oka et al. 1999). In section 3.3, we detect no significant temperature variations on $\sim 2'$ scales.

3.5. Cloud masses

To estimate the total cloud masses from their integrated fluxes, we require the grain absorption cross-section per unit mass of gas and dust. We have adopted the parameters suggested by Pollack et al. (1994) with opacity index $\beta = 2$, and a correction for Galactic Centre metallicity $Z/Z_\odot = 2$ (Mezger et al. 1989). We thus derive opacities of $\kappa_{450\mu\text{m}} = 4.94 \times 10^{-3} \text{ m}^2 \text{ kg}^{-1}$ and $\kappa_{850\mu\text{m}} = 1.38 \times 10^{-3} \text{ m}^2 \text{ kg}^{-1}$. Assuming a uniform dust temperature of 20 K we have for $\lambda = 450$ and 850 μm , conversion factors of 63.3 and 513 M_\odot/Jy respectively. The total mass found by the survey, measured by integrating the total 850 μm brightness, is then $(53 \pm 10) \times 10^6 M_\odot$.

The largest source of error in these mass measurements is our uncertainty of the dust temperature. The value of 20 K is derived in section 3.3, but Lis, Carlstrom, & Keene (1991) adopt a mean temperature of 30 K. However, the ISO study of GCM0.25+0.01 by Lis & Menten (1998) gives a mean temperature of ~ 18 K for this core, suggesting that the lower dust temperatures are correct.

We neglect optical depth effects as the emission is optically thin at $850\,\mu\text{m}$ except from Sgr B2.

4. Further discussion

The improved depth, resolution, and extent of the SCUBA survey reveal many new features in the Galactic Centre. Not only are there the known large star-forming cloud complexes but also a wide-ranging network of dusty filaments is revealed. For example, at negative Galactic longitudes close to $b = 0$ there is filamentary structure which may be continuous and stretches along the Galactic plane for up to 0.8° (120 pc). There are partial shells, possibly associated with the known SNRs Sgr A East (G0.0+0.0), G0.3+0.0, G0.9+0.1, and G1.4-0.1 (Green 1998). There is also a circular shell of dust clouds centred on $l, b = (0.8, -0.18)$ which does not appear to be documented, and which we have labelled PPR G0.80-0.18. This may trace a wind-blown region or perhaps a supernova remnant. In a future paper, we will contrast these structures with star-forming regions near the Solar circle, comparing masses, densities, dust grain properties and star-forming efficiency.

The total mass detected by our survey is $(53 \pm 10) \times 10^6 M_\odot$, in the inner 400 pc. Dahmen et al. (1998) derived a weighted best estimate of the total mass in the inner 600 pc of the Galactic centre using a combination of dust emission, gamma rays, and C^{18}O molecular line emission. This estimate was $20\text{--}50 \times 10^6 M_\odot$. The best optically-thin tracer in this set is the C^{18}O survey, from which was derived a mass of $17 \times 10^6 M_\odot$ in the central 600 pc. Although our survey covers a smaller area, the total mass detected is significantly greater. Therefore, the SCUBA data comprise the first optically-thin map to trace essentially all the mass in the CMZ at high resolution.

We are grateful to the UK Panel for Allocation of Telescope Time for the award of observing time for this project. JSR acknowledges a Royal Society Fellowship and DP-P a PPARC Research Studentship. The JCMT is operated by the Joint Astronomy Centre on behalf of PPARC of the UK, the Netherlands OSR, and NRC Canada. We acknowledge the support provided by the Starlink Project which is run by CCLRC on behalf of PPARC. We also would like to thank an anonymous referee for some very useful comments.

REFERENCES

Agladze, N. I., Sievers, A. J., Jones, S. A., Burlitch, J. M., & Beckwith, S. V. W. 1996, *ApJ*, 462, 1026+

Aitken, D. K., Greaves, J., Chrysostomou, A., Jenness, T., Holland, W., Hough, J. H., Pierce-Price, D., & Richer, J. 2000, *ApJ*, 534, L173

Bernard, J. P., et al. 1999, *A&A*, 347, 640

Cao, Y., Terebey, S., Prince, T. A., & Beichman, C. A. 1997, *ApJS*, 111, 387+

Dahmen, G., Huttemeister, S., Wilson, T. L., & Mauersberger, R. 1998, A&A, 331, 959

Dent, W. R. F., Matthews, H. E., Wade, R., & Duncan, W. D. 1993, ApJ, 410, 650

Dowell, C. D., Lis, D. C., Serabyn, E., Gardner, M., Kovacs, A., & Yamashita, S. 1999, in ASP Conf. Ser. 186: The Central Parsecs of the Galaxy, 453+

Draper, P. W., Taylor, M., & Allan, A. 2000, Starlink User Note 139, Rutherford Appleton Laboratory

Green, D. A. 1998, A Catalogue of Galactic Supernova Remnants (1998 September version) (Mullard Radio Astronomy Observatory, Cambridge, United Kingdom)

Holland, W. S., et al. 1999, MNRAS, 303, 659

Jenness, T. & Lightfoot, J. F. 1998, in ASP Conf. Ser. 145: Astronomical Data Analysis Software and Systems VII, Vol. 7, 216+

Jenness, T. & Lightfoot, J. F. 1999, Starlink User Note 216, Rutherford Appleton Laboratory

Koike, C., Kimura, S., Kaito, C., Suto, H., Shibai, H., Nagata, T., Tanabe, T., & Saito, Y. 1995, ApJ, 446, 902+

Lis, D. C. & Carlstrom, J. E. 1994, ApJ, 424, 189

Lis, D. C., Carlstrom, J. E., & Keene, J. 1991, ApJ, 380, 429

Lis, D. C. & Menten, K. M. 1998, ApJ, 507, 794

Lis, D. C., Menten, K. M., Serabyn, E., & Zylka, R. 1994, ApJ, 423, L39

Lis, D. C., Serabyn, E., Keene, J., Dowell, C. D., Benford, D. J., Phillips, T. G., Hunter, T. R., & Wang, N. 1998, ApJ, 509, 299

Mezger, P. G., Zylka, R., Salter, C. J., Wink, J. E., Chini, R., Kreysa, E., & Tuffs, R. 1989, A&A, 209, 337

Morris, M. & Serabyn, E. 1996, ARA&A, 34, 645

Oka, T., Hasegawa, T., Sato, F., Tsuboi, M., & Miyazaki, A. 1998, ApJS, 118, 455

Oka, T., White, G. J., Hasegawa, T., Sato, F., Tsuboi, M., & Miyazaki, A. 1999, ApJ, 515, 249

Pollack, J. B., Hollenbach, D., Beckwith, S., Simonelli, D. P., Roush, T., & Fong, W. 1994, ApJ, 421, 615

Serabyn, E., Carlstrom, J., Lay, O., Lis, D. C., Hunter, T. R., & Lacy, J. H. 1997, ApJ, 490, L77

Tsuboi, M., Miyazaki, A., & Tsutsumi, T. 1999, in ASP Conf. Ser. 186: The Central Parsecs of the Galaxy, 105+

Zylka, R., Mezger, P. G., Ward-Thompson, D., Duschl, W. J., & Lesch, H. 1995, A&A, 297, 83

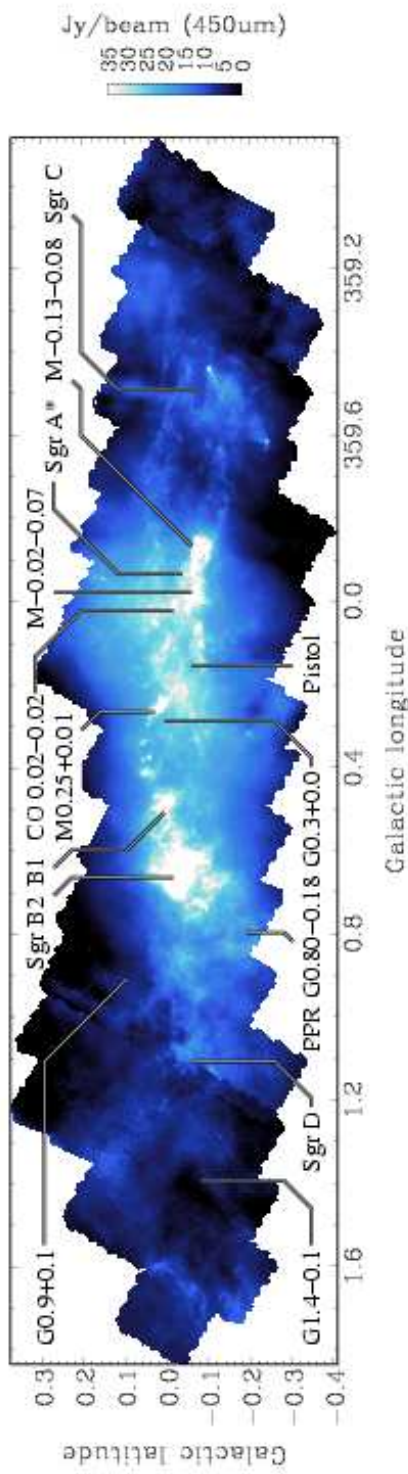


Fig. 1.— SCUBA Galactic Centre Survey: 450 μ m flux density.

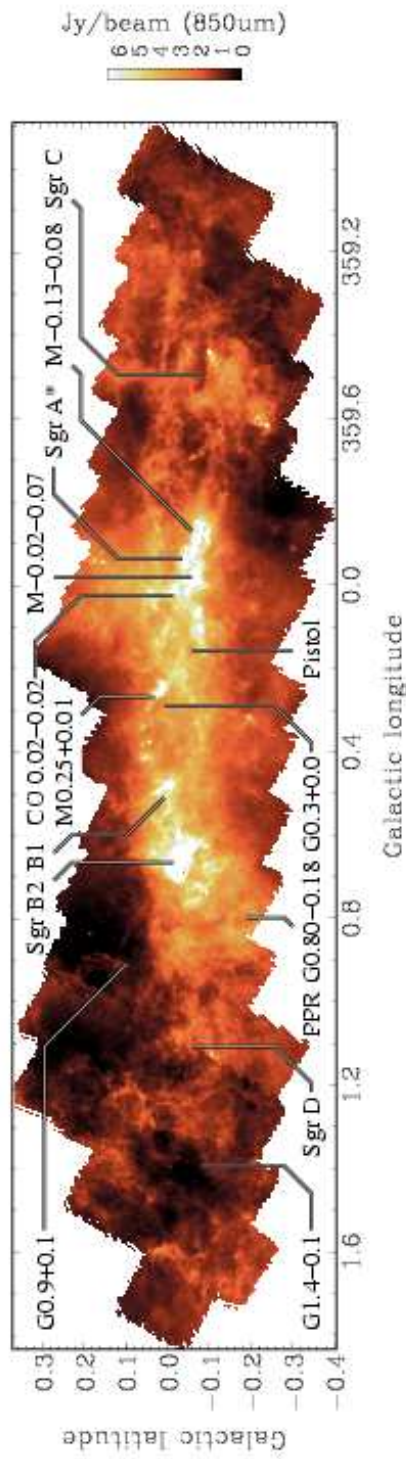


Fig. 2.— SCUBA Galactic Centre Survey: 850 μ m flux density.

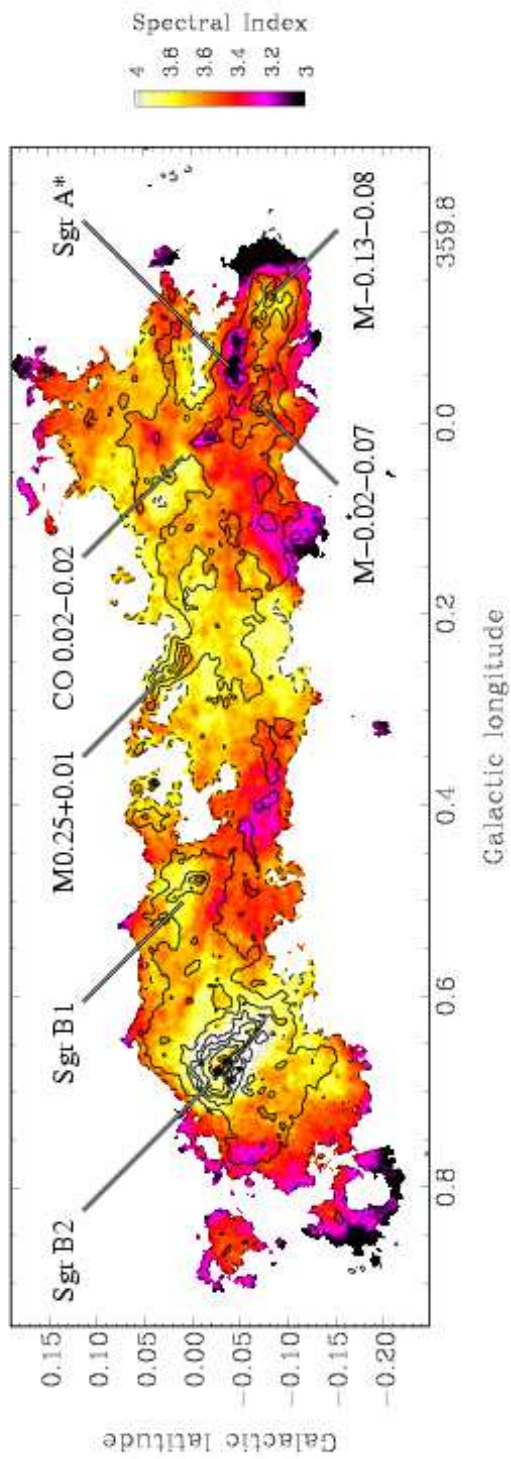


Fig. 3.— Spectral index map for central region, with contours of $850\mu\text{m}$ map.